

Thermal Performance Enhancement of Asphalt Solar Collector by Using Extended Surfaces

Firas A. Abbaa^{1*}, Mohammed H. Alhamdo²

¹ Chief Engineer, Ministry of Oil, S.C.G.F.S / Wassit, Iraq

² Mustansiriyah University, College of Engineering, Mech. Eng. Dept., Baghdad, Iraq

Corresponding Author Email: laithfiras3@gmail.com



<https://doi.org/10.18280/psees.050104>

ABSTRACT

Received: 26 November 2021

Accepted: 19 December 2021

Keywords:

asphalt solar collector, extended surfaces, embedded tubes, urban heat island

The Urban Heat Island (UHI) effect occurs when the temperature of the asphalt pavement surface exceeds 70°C during the summer. Rutting is a significant temperature-related problem that occurs when the temperature rises too high on asphalt surfaces. Additionally, this phenomenon increases the amount of energy required to cool buildings adjacent to pavements and degrades air quality. The Asphalt Solar Collector (ASC) was examined in this work by inserting tubes into the pavement's construction and circulating working fluid within it to capture thermal energy generated by asphalt pavement. A low-carbon steel-alloy cheap waste materials have been investigated as an extended surface with HMA. The effect of various extended surfaces attached to the embedded tubes on the thermal performance of ASC has been studied to determine whether it satisfies specified aforementioned demands. The performance of several ASC models with bare, continuous finned, and mesh grid serpentine embedded tubes was investigated with same Conductive Hot Mixture Asphalt (C-HMA) by using a numerical 3-D model developed by COMSOL Multiphysics Software. when the Reynolds Number is increased, it is found that ASC efficiency increases from 66.74% for bare serpentine tubes to approximately 75.488% and 69.4% for continuous finned and mesh grid serpentine embedded tubes, respectively. A maximum value of about 398.53 W can be gained (from a total of 850 W/m² incident solar radiation) by utilizing an extended surface. Additionally, the surface temperature of HMA decreases significantly from 52.67 to 46.07°C. For all models under investigation, it is clear that the optimum average Reynolds Number is about 600. It is found that the continuous fins model can capture more solar radiation than the mesh grid model by about 8.77%.

1. INTRODUCTION

The earth's surface absorbs around half of the solar energy that strikes the planet [1]. The most often utilized type of road paving is asphalt. They can be heated to 70°C in the summer by solar radiation due to their great absorption capacity [2, 3]. The infrastructure is made up of paved areas such as roads, pathways, and garages. The elevated temperatures generated from HMA cause a variety of problems, including the UHI effect, which may be uncomfortable for people, and pavement deterioration, such as rutting [4-6]. UHI possesses detrimental effect on air quality besides increasing energy demand for cooling buildings adjacent to pavements [4]. Additionally, rutting is a serious temperature-related problem that occurs when the temperature rises too high in asphalt surfaces [6]. By lowering the pavement temperature, heat collected from the pavement through embedded tubes may also contribute to alleviate the UHI effect and rutting potential of the pavement [2, 5]. The temperature of the pavement is determined by the energy balance between the heat source's irradiation and the heat absorbing surface, transporting, and storing capacities of the HMA. Heat is transferred by conduction, radiation, and convection [7].

ASC are consisted of embedded tubes that circulating a fluid. Solar radiation raises the temperature of the pavement. The temperature differential between the fluid moving through

tubes and the pavement causes heat to be transferred from the pavement to the fluid, resulting in a decrease in pavement temperature and a rise in fluid temperature. Reduced asphalt temperature has a beneficial effect on reducing the impact of UHI and the occurrence of permanent deformation. What makes ASC so desirable is its ability to produce energy from the heat generated by the flowing fluid's temperature increase [8]. As illustrated in Figure 1, an ASC is made of three distinct material media: two solids, the asphalt pavement and tubes, and two fluids, the ambient air and the fluid running through the tubes. Conduction, convection, and radiation all contribute to heat transmission in an ASC. At first, the energy is balanced at the pavement-atmosphere interface. Solar radiation, convection, and thermal radiation all participate to the heat transfer across this contact. This heat flux results in a temperature differential between the asphalt surface and a place deep beneath the pavement, which results in conduction from the surface to the interior. At the depth of the buried tubes, conduction heat transmission continues through the pavement-tube contact and the tube wall. Convection occurs when the temperature difference between the tube's inner surface and the fluid results in an increase in the fluid's temperature [8, 9].

A hybrid material assembly HMA is a composite material consisting of aggregates, bitumen, and air voids. It is one of the most often used materials in the world's pavement building. When solar energy is received by a pavement, it may be

transported or stored in the materials, depending on their properties [10]. Due to the fact that asphalt pavement is exposed to solar radiation throughout the day, it may collect a significant amount of solar energy, which is subsequently converted to thermal energy inside the pavement structure. On the one hand, this phenomenon has an effect on the durability of asphalt pavements [11, 12]. High temperatures, as a consequence of traffic, will permanently deform asphalt pavement. Additionally, it might accelerate thermal oxidation, impairing the performance of the pavement. On the other hand, a greater pavement surface temperature has an adverse effect on the environment. The development of the UHI effect, which indicates that the temperature in the urban area is greater than in the surrounding suburban and rural regions, is effected by the high surface temperature [11].

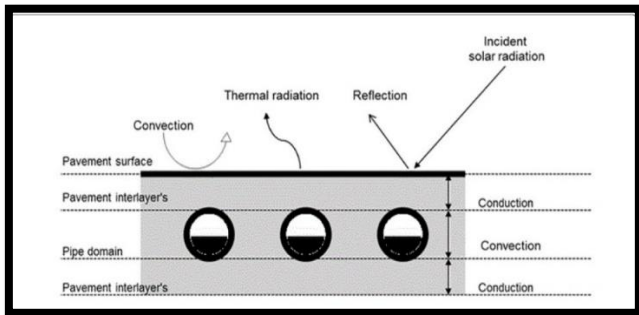


Figure 1. Heat transfer mechanisms in an ASC [9]

Extended surfaces have been used to transport heat between low and high thermal resistance zones in single and two-phase systems. The finned tube performance is limited by its low thermal resistance side. This is because the thermal properties of this side are much lower than the heat transfer coefficient of the opposite side. On the liquid side of these tubes, the thermal properties are generally one order of magnitude greater than on the high thermal resistance side. Extended surfaces are used on the side with a high thermal resistance to increase the surface area, allowing for balanced thermal conductance on both sides of a heat exchanger [13].

Wire meshes are lightweight and dense structures with excellent permeability and thermal conductivity, making them ideal for a broad variety of industrial applications that involve fluid flow and heat transfer. Due to their low weight, large surface area to volume ratio, high strength to weight ratio, and excellent thermal conductivity, wire meshes may also be used as fins to promote heat transmission in heat exchangers. Metallic wire meshes are porous materials made out of a mesh of metals arranged in square, rectangular, or circular patterns. A range of pore sizes, wire diameters, and wire kinds are available in wire mesh screens [14].

In theoretical ASC research, the Finite Element Method (FEM) is often employed, whereas the Finite Difference Method (FDM) is frequently used in pavement thermal evaluation. While ANSYS Software is the most widely used commercial software tool for performing finite element thermal analysis, other packages such as FEMMASSE and COMSOL are also useful.

In the literature, theoretical research utilizing numerical modeling and simulation has been used to examine the behavior of an ASC. Bijsterveld et al. performed thermal analyses using data from a field test in northern Netherlands, where polyethylene tubes were installed to regulate pavement

temperature along a vital route. They concluded from the investigation's results that energy extraction from asphalt pavements comprises plenty of complex technical and economic difficulties that must be resolved before effective use can occur. Wu et al. [15] used the harvesting of solar energy to make a full-depth asphalt surface. In their work, they used numerical modeling and experimental investigation to confirm the vertical temperature distribution of a full-depth asphalt slab [16-19]. The results demonstrated that the numerical model can be used to predict the vertical temperature distribution of asphalt pavement while also reducing the cost and energy associated with the experiments, demonstrating that the testing results were valid and serving as a computational reference for pavement engineers. Nicolas and Eleftherios [20] investigated the use of an ASC for heat capture and a ground source heat pump with borehole storage to satisfy home hot water and heating needs in a newly designed residential area. The ASC was designed using the numerical modeling program COMSOL Multiphysics, while the ground source heat pump and borehole storage system were controlled using Earth Energy Designer 3 (EED3) (EED3). Following a thorough economic and environmental analysis, a global design of the system was applied to meet the system's energy requirements. They obtained several findings on the system's overall performance and utility [2]. Basheer and Krishnan (2014) incorporated thermal and structural study of an ASC using the finite element method. Under the specified circumstances, various models were utilized to calculate the optimal tube spacing, diameter, depth, and arrangement. They determined that the depth and spacing of the tubes significantly affect the temperature distribution inside the pavement. Within a certain range, the structural stability was not significantly affected. They concluded as a result that the structural and thermal properties of ASC varied according to the ambient temperature, mix proportions, and compactness of the pavement. Only via real-time testing on large models could accurate performance be predicted. Nasir et al. conducted an investigation into optimizing the road pavement solar collector (RPSC) system using four parameters (tube diameter, tube depth, water velocity, and water temperature), comparing system performance in terms of inlet-outlet Delta T, potential thermal collection (PTC), and surface temperature reduction (STR). The external environment's (macro domain) influence on the RPSC system (micro domain) was modelled utilizing a decoupled CFD technique in two separate CFD models. When compared to other simulated parameters, they found that the system change based on high and low water velocity conditions resulted in the best performance gain, with an average increase of 28% in PTC and STR. However, with a tube diameter greater than 0.02 m and a water velocity of 0.25 m/s, a minimum Delta T (less than 5 K) was attained. Khoja and Waheeb [9] investigated the effectiveness of a simulated 20 m² ASC for three low to medium-temperature solar thermal applications in hot and humid areas, namely sun aided cooling, atmospheric water generation, and household hot water. The performance of ASC in hot humid circumstances was investigated using TRNSYS simulations. They validated the developed TRNSYS model's validity by comparing its performance to empirical data from the case study city. According to their sensitivity analysis findings, installing a road-rated heat insulating layer beneath the tube-carrying asphalt layer improved ASC performance. Chiarelli et al. performed experimental testing and computational fluid dynamics (CFD) simulations to

identify how to optimize the design of a convection-powered ASC prototype for the purpose of reducing high urban pavement temperatures. They evaluated an energy harvesting system that employs buried tubes to a projected design style that uses concrete corrugations to replace the tubes. CFD models were used to optimize the air collecting chamber, which was placed just before the warm air leaves the ASC prototype. Energy and exergy were calculated from the collected data. For optimal performance, tubes should be installed in a single row under the pavement wearing course. This resulted in a surface temperature drop of up to 5.5°C and the greatest levels of absorbed energy and exergy in the pavement prototype studied. Additionally, CFD simulations indicated that the shape and size of the air collecting chamber must be carefully selected, since they have a significant effect on the system's behavior. Ahmed calculated solar heat temperature fluctuations in copper and rubber tubes embedded under asphalt pavement using the finite element technique. In the asphalt surface, copper and rubber tubes were placed in a serpentine pattern. ANSYS was used to model 300 x 300 and 300 x 500 mm asphalt pavements. Copper and rubber serpentine tubes with a diameter of 40 mm were embedded in the asphalt surface. The solar heat temperature was collected in asphalt at depths of 50, 100, and 150 mm. Their findings revealed that asphalt pavements with a larger exposed surface area (300 x 500 mm) collect more energy than asphalt pavements with a smaller exposed surface area (300 x 300 mm). The serpentine configurations of copper and rubber tubes embedded in asphalt pavement collected solar heat slightly different. Solar heat was captured at a higher rate at 50 mm depth than at 100 and 150 mm depths. Hasan et al. investigated the effect of tube configuration on heat dynamics and ASC performance using experimental and numerical analyses. The findings indicated that by arranging the tubes properly, the thermal efficiency of the ASC may be increased by up to 70%, while the output temperature rises by around 10% [19].

It is clear all previous works that examined the use of road pavements as energy collectors in recent years, developing a range of technologies and approaches. These studies are primarily concerned with the generation of energy from the heat collected by pavements. However, on the other hand, the effects of using extended surfaces to the tubes remain to be addressed in order to better understand the thermal phenomena inside ASC.

Therefore, the main aim of this paper is to examine the influence of various extended surfaces attached to the outer surface of embedded tubes on the performance of an ASC. Specifically, by using low carbon steel wastes to create continuous fins or a mesh grid. COMSOL Multiphysics 5.6.0.280, shall be used to investigate the thermal effects of serpentine embedded tubes with and without extended surfaces to determine the performance enhancement of various ASC models.

2. MATHEMATICAL MODELING AND NUMERICAL SIMULATION

As a beginning, a 3D model of the HMA and fluid domain is created using SOLID WORKS S 2021. The model is then loaded into the COMSOL software for thermal analysis. The model contains an ASC with bare or finned serpentine

embedded tubes of inlet and outlet portions. The HMA's lateral and bottom faces are insulated, except for the upper side, which is exposed to solar radiation. The computational domains in this study are represented by the inlets and outlets of water in the embedded tubes inside HMA. Solar radiation strikes the upper face of HMA, as depicted in Figure 2.

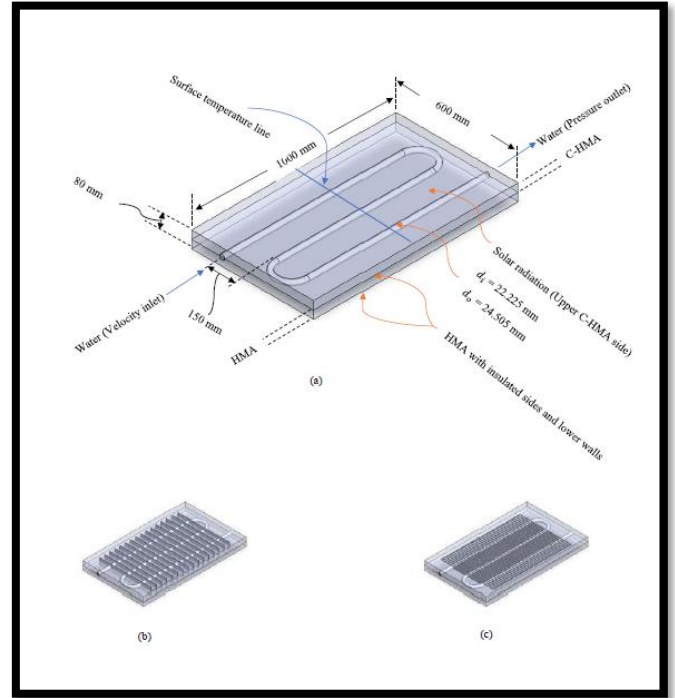


Figure 2. Basic design of ASC with serpentine embedded tubes: (a) Bare. (b) Continuous finned. (c) Mesh grid

The assumptions made for ASC in this study are that both the HMA and embedding tubes are completely homogeneous, isotropic, and uniform, temperature changes in the direction of the embedded tube are uniform, heat resistance between layers is ignored because the contact between adjacent layers is sufficiently close, temperature and heat flux between layers are completely continuous, Newtonian and incompressible fluids are maintained inside the embossed tube, Three-dimensional model, laminar flow within embedded tubes on the water side, the buoyancy effect is assumed insignificant, and the water side does not contain radiation heat transfer.

The preceding sections discussed the governing equations for ASC [20].

Asphalt domain

$$\rho_{HMA} c p_{HMA} \frac{\partial T_{HMA}}{\partial t} + \nabla \cdot (-K_{HMA} \nabla T_{HMA}) = 0 \quad (1)$$

Boundary condition for HMA surface and bottom respectively:

$$\begin{aligned} -n \cdot (K_{HMA} \nabla T_{HMA}) &= \alpha G_o + h_{amb} (T_{amb} - T_{HMA,S}) \\ &+ \epsilon \sigma T_{HMA,S}^4 \end{aligned} \quad (2)$$

$$(-K_{HMA} \cdot \nabla T_{HMA}) = 0 \quad (3)$$

Table 1. Details of optimum number of elements for various studies

ASC type	No. of Elements	Element type		Triangles	Quads	Min. Element quality	Ave. Element quality
		Tetrahedra	Prisms				
Continuous finned serpentine tubes	2722687	2535643	187044	374791	5760	0.02219	0.663
Mesh grid serpentine tubes	3896142	3661438	234704	450272	5456	0.0743	0.6644

Water domain

$$\rho_w c p_w \frac{\partial T}{\partial t} + \nabla \cdot (-K_w \nabla T_w) = -\rho_w C_{u,w} \cdot \nabla T_w \quad (4)$$

Boundary condition for water inlet and outlet respectively:

$$T_w = T_{w1} \quad (5)$$

$$(-K_w \cdot \nabla T_w) = 0 \quad (6)$$

Asphalt – water domain

$$\begin{aligned} &(-K_w \cdot \nabla T_w + \rho_w \cdot c p_w \cdot u_{w,y} \cdot T_w) \\ &- (-K_{HMA} \cdot \nabla T_{HMA}) = 0 \end{aligned} \quad (7)$$

The collector model was meshed using the Module Builder's Physics-Controlled mesh. As illustrated in Figure 3, the Physics-Controlled tool refined meshing for all domains in the ASC. Grid refinement research was undertaken to ensure that the numerical simulation's result is not affected by the grid's non-uniform resolution. The outlet water temperature of the embedded tubes has been explored during this study to establish the appropriate number of elements necessary due to the important role of this parameter in the thermal performance of ASC at 0.09 m/s water inlet velocity and 1000 W/m² solar radiation. The convergence study in ASC with diverse scenarios are illustrated in Figures 4 and 5. The output water temperature of ASC with continuous finned and mesh grid serpentine embedded tubes begins to decline as the number of elements grows up to 2722687 and 3896142 respectively. After that, the outlet temperature is approximately linear and does not change considerably as the number of elements rises. Table 1 gives more information of recommended mesh density in these cases.

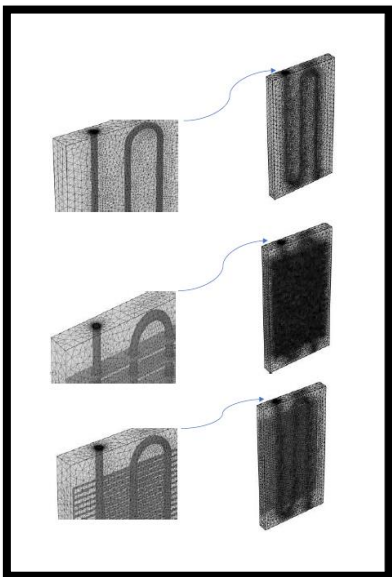


Figure 3. An example of the mesh that was used in this research

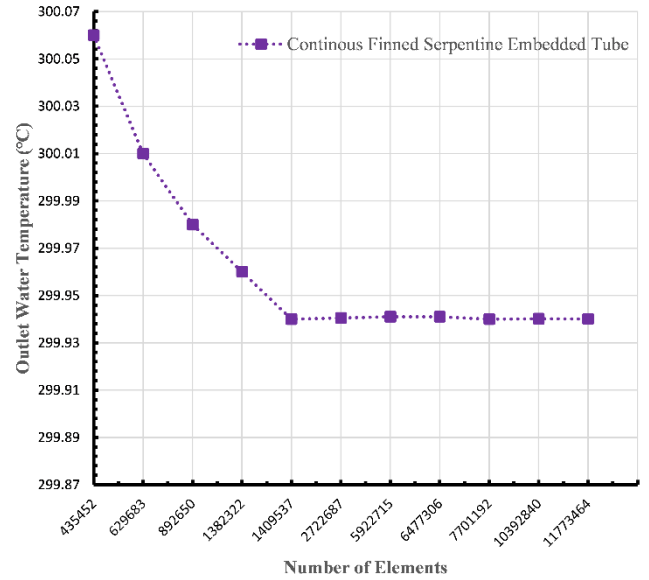


Figure 4. Effect of number of elements on the outlet water temperature of ASC with continuous finned serpentine embedded tubes

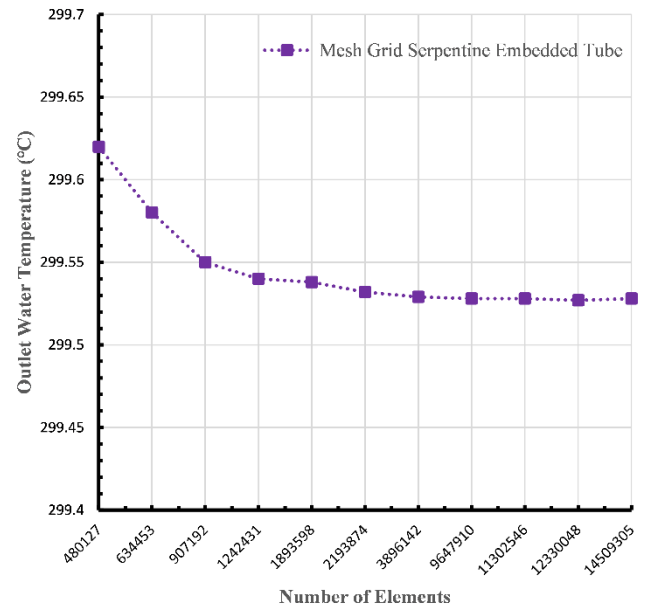


Figure 5. Effect of number of elements on the outlet water temperature of ASC with mesh grid serpentine embedded tubes

3. MODEL VALIDATION

To validate the COMSOL Multiphysics 5.6.0.280 software used during the study, the Jinshah et al. model was numerically examined utilizing current program rather than their COMSOL Multiphysics 4.3b software. The identical boundary

conditions as those employed previously by the researchers were used in this simulation. When compared to the results of Jinshah et al., the developed numerical model is found to accurately estimate heat transfer and fluid flow in the simulation of Jinshah model with a 1.47% error, as illustrated in Figure 6.

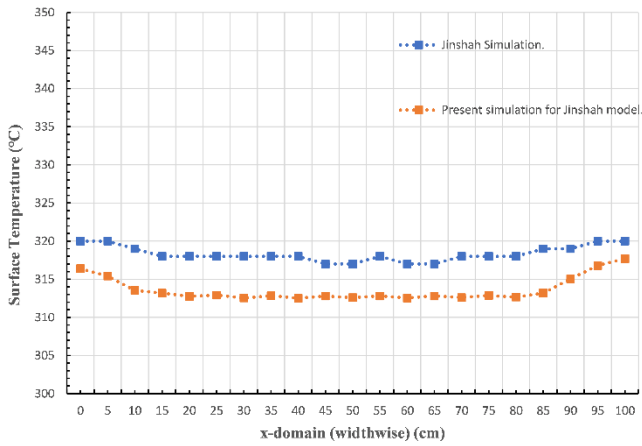


Figure 6. Validation of numerical simulation

4. THERMAL ANALYSIS

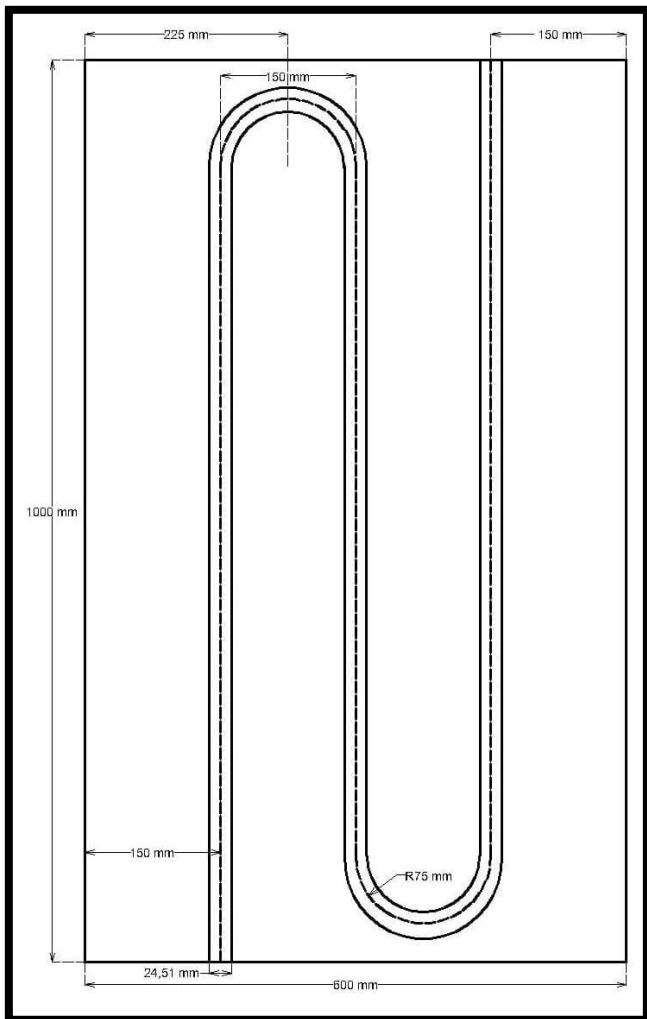


Figure 7. ASC with serpentine embedded tubes

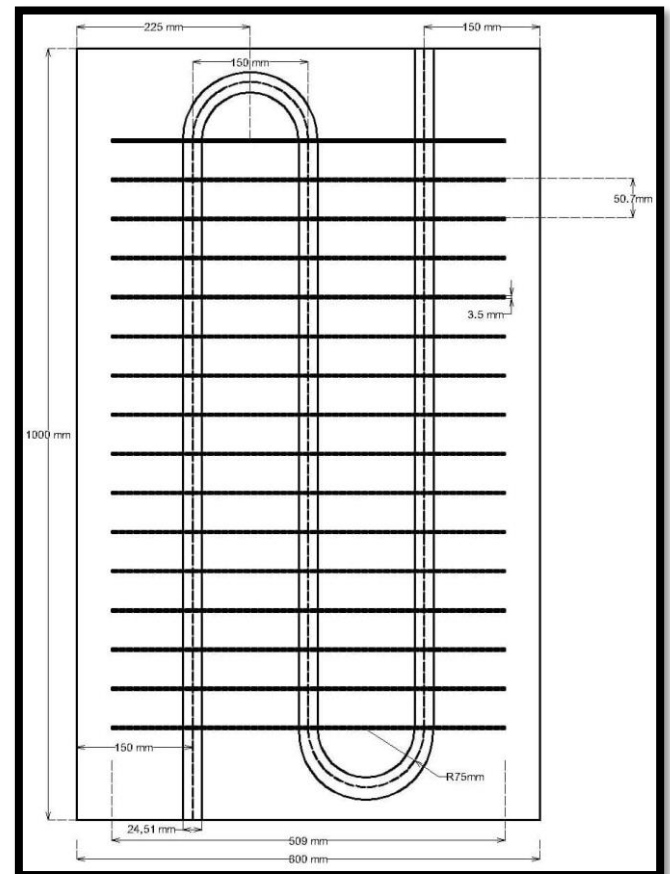


Figure 8. ASC with continuous finned serpentine embedded tubes

Simulations have been conducted on various models with bare, continuous finned, and mesh grid serpentine embedded tubes to determine the temperature change within the asphalt pavement and the amount of energy taken by the circulating water. Figures 7, 8, and 9 illustrate the ASC structure that was chosen for this investigation. The pavement construction is 1000 mm x 600 mm and has an overall depth of 80 mm. The structure consists of two layers, as illustrated in Figure 2. The reference mixture was maintained in the lower layer, while the enhanced mixtures in the upper layer. This is because it was determined that there is no noticeable thermal effect through the lower layer in comparison to the effect expected from the upper layer exposed to solar radiation from one hand and water tubes from the other hand. The asphalt mixtures utilized in this study and their thermophysical properties are listed in Tables 2 and 3 respectively. The ASC is studied by varying solar radiation, and water velocity while maintaining the other conditions constant for various extended surfaces on embedded tubes. Thermal analysis is performed using the Heat Transfer Module in COMSOL Multiphysics 5.6.0.280. The present study involves model the Conjugate Heat Transfer-Laminar Flow Interface. This model is generally used to simulate slow-moving flow in contexts where temperature and energy transport are also critical components of the system and must be coupled or related in some way to the fluid flow. Separate fluid domains were chosen, and the substance was assigned to be water. Copper was chosen as the tube material for the ASC due to its excellent thermal conductivity. The user interface is made of copper and has a layer thickness of 1.14 mm. Table 4 shows the various input circumstances for analysis.

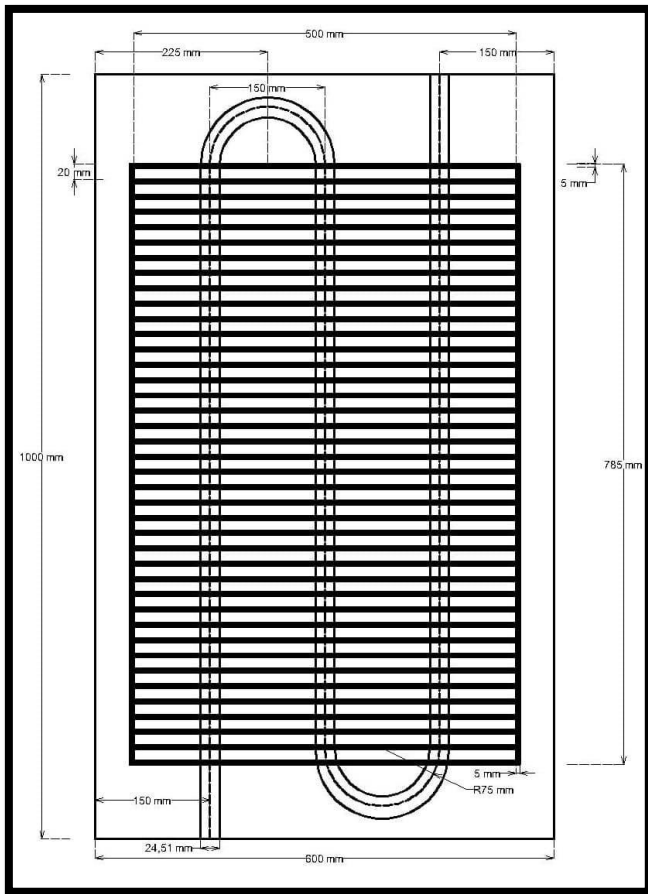


Figure 9. ASC with mesh grid serpentine embedded tubes

Table 2. The asphalt mixtures that were employed in the investigation

No.	Mixes	Description
1	RHMA	The aggregates used in the mix were entirely limestone.
2	SSt.HMA	Slag stone aggregates (5-12) mm replaced limestone aggregates; Silica sand replaced normal fine aggregates; Slag filler replaced limestone filler; (4%) by binder volume Steel wool fibers as additives ;30% addition from the original binder percentage of mixing equation added in RHMA

Table 3. Asphalt mixes' thermophysical properties

No.	Mixes	K ($\frac{W}{m.K}$)	c_p ($\frac{J}{kg.K}$)	ρ ($\frac{kg}{m^3}$)	$\alpha(10^{-7})$ ($\frac{m^2}{s}$)
1	Reference HMA	1.161	919.55	2337	5.4
2	SSt.HMA	2.482	767.79	2337	1.383
3	Copper tube	400	385	8700	1.19
4	Low carbon steel extended surfaces	53	470	7900	1.4

Table 4. Details of the input for the thermal analysis in COMSOL

No.	Boundary condition	details
1	Initial temperature	$T_{initial} = 298 \text{ K}$
2	Surface to ambient radiation	$\epsilon = 0.95 T_{amb} = 298 \text{ K}$

3	Heat flux input	450-850 W/m^2 overall inward heat flux condition at the model's top surface
4	Thermal Insulation	Insulated bottom and side surfaces
5	Pipe wall condition	There is no boundary slip condition.
6	Convective heat flux	The heat transfer coefficient specified by the user is $5 \text{ W/m}^2, k$ on the top surface, with $T_{amb}=298\text{K}$.
7	Water inlet temperature	$T_i = 298 \text{ K}$
8	Inlet water velocity	0.01m/s – 0.09 m/s

5. RESULTS AND DISCUSSIONS

For various extended surfaces on embedded tubes, preliminary parametric study is undertaken on water velocity and solar radiation. The heat transfer module was used to determine the thermal behavior of each mesh node in COMSOL Multiphysics. This study is concerned with the amount of heat that can be gathered and the expected outlet temperature. The meteorology input data is derived from real-time weather data collected in Baghdad, Iraq. Figure 10 depicts the post-processing of temperature values for each mesh point in the models.

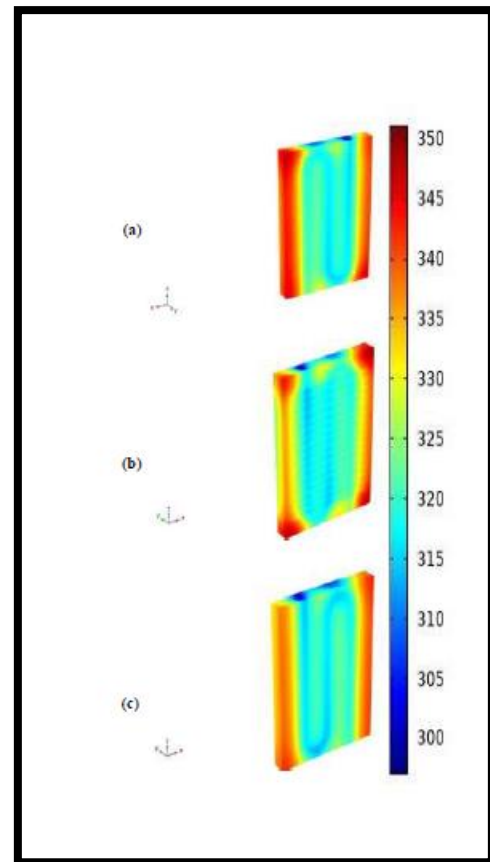


Figure 10. COMSOL Multiphysics temperature solution for ASC at water velocity = 0.03 m/s and solar radiation = 850 W/m^2 with: (a) Serpentine embedded tubes. (b) Continuous finned serpentine-embedded tubes. (c) Mesh grid serpentine-embedded tubes

As illustrated in Figure 10-a, the placement of the embedded

tubes within ASC certainly contributed to their temperature reduction. Figure 10-b, c indicates the effects of extended surfaces on ASC performance.

The thermal behavior of the model in Figure 10 can be also observed by Figures 11, 12, and 13. Each figure involves an increase in the temperature of the working fluid over the length of the embedded tubes due to the variation of Reynolds Number. Continuous finned and mesh grid tubes exhibit outlet temperatures of 32.94 C and 32.3 C, respectively, compared with 32.02 C for bare serpentine tubes at Reynolds Number of 746. Increased ASC efficiency is achieved by increasing the water Reynolds number inside embedded tubes. When the Reynolds Number is increased, it is found that ASC efficiency increases from 66.74% for bare serpentine tubes to approximately 75.488% and 69.4% for continuous finned and mesh grid serpentine embedded tubes, respectively.

The relationship between thermal energy gain and water velocity in ASC using bare, continuous finned, and mesh grid serpentine embedded tubes is illustrated in Figure 14. Thermal energy is gradually gained as the velocity of the water increases. A maximum value of about 398.53 W can be gained (from a total of 850 W/m² incident solar radiation) by utilizing an extended surface.

For all models under investigation, it is clear from Figures 11 to 13 that the optimum average Reynolds Number is about 600.

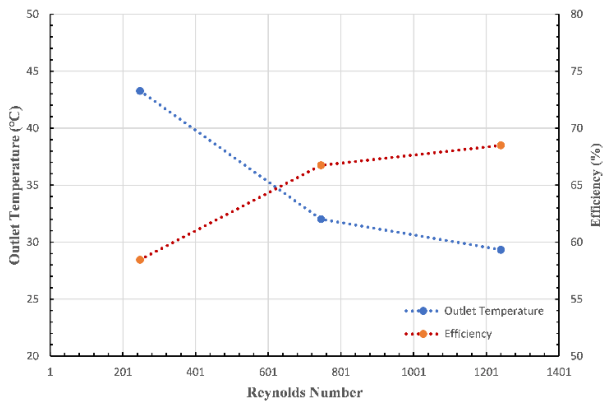


Figure 11. Outlet temperature and solar efficiency as a consequence of water Reynolds Number for serpentine tubes at water velocity = 0.03 m/s and solar radiation = 850 W/m²

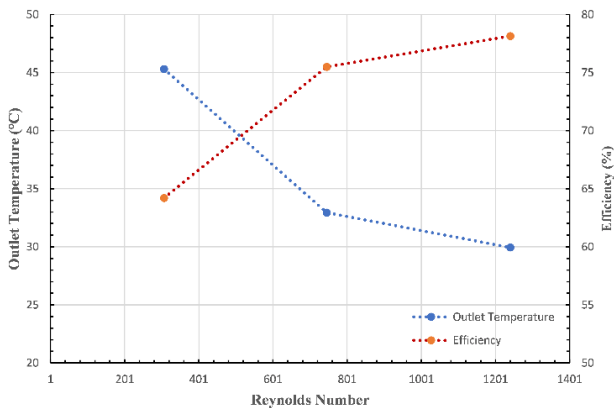


Figure 12. Outlet temperature and solar efficiency as a consequence of water Reynolds Number for continuous finned serpentine tubes at water velocity = 0.03 m/s and solar radiation = 850 W/m²

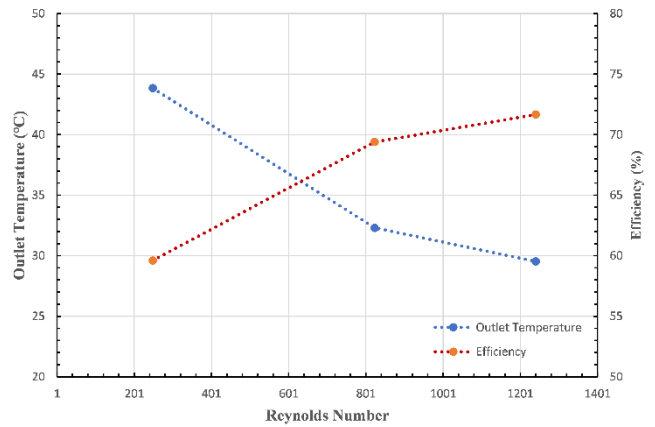


Figure 13. Outlet temperature and solar efficiency as a consequence of water Reynolds Number for mesh grid serpentine tubes at water velocity = 0.03 m/s and solar radiation = 850 W/m²

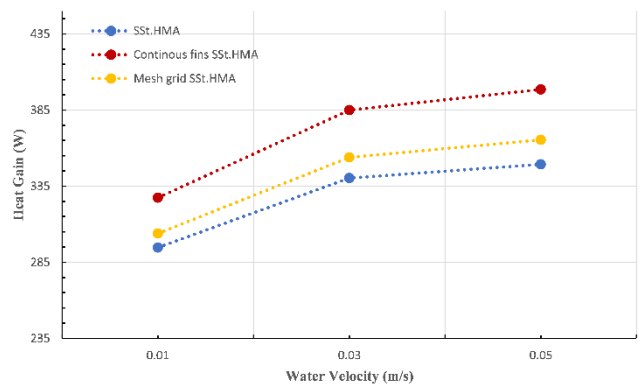


Figure 14. Variation of water velocity with heat gain of various cases of extended surfaces at solar radiation = 850 W/m² for various HMA types

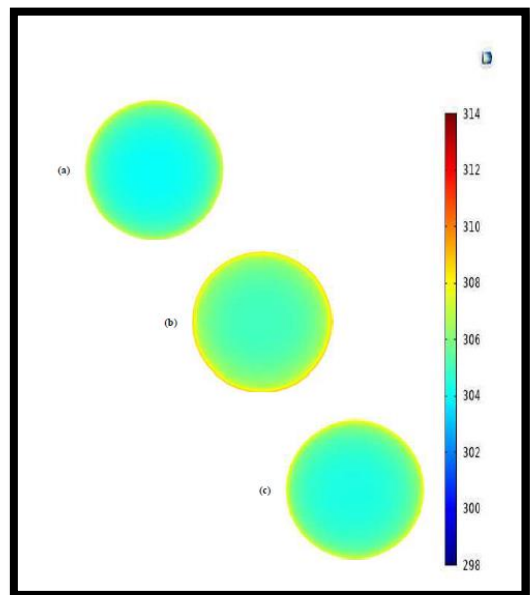


Figure 15. Surface average of outlet temperature contours at water velocity = 0.03 m/s and solar radiation = 850 W/m² with: (a) Bare serpentine-embedded tubes. (b) Continuous finned serpentine-embedded tubes. (c) Mesh grid serpentine-embedded tubes

The surface average for the water exit area at the end of the serpentine embedded tube is shown in Figure 15, demonstrating the rise in outlet water temperature achieved by employing embedded tubes' surface area enhancement.

The temperature change within continuous fins and a mesh grid solved using COMSOL is illustrated in Figures 16 and 17. The cross section of Figure 18 illustrates the effect of extended surfaces on the temperature gradient in HMA and the priority of continuous fins towards reducing the temperature inside the asphalt mixture.

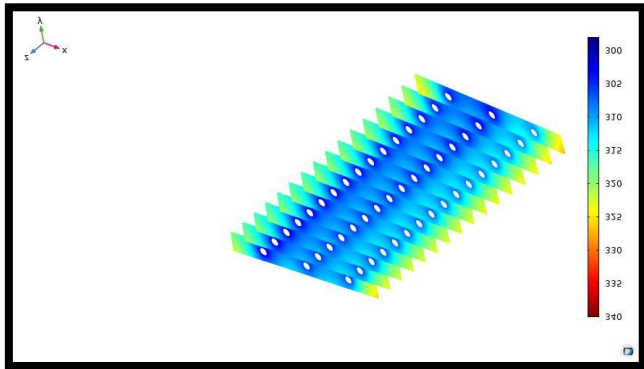


Figure 16. Temperature change within continuous fins at water velocity = 0.03 m/s and solar radiation = 850 W/m²

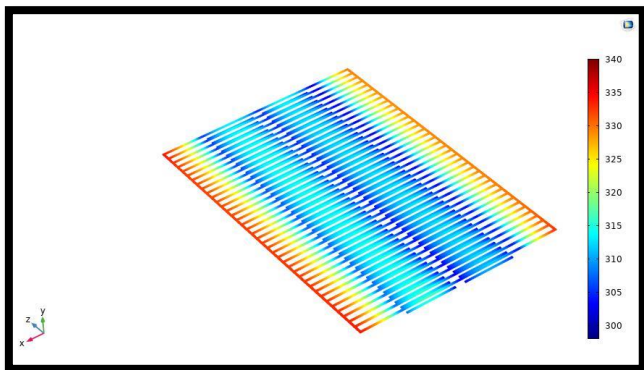


Figure 17. The distribution of temperature within mesh grid at water velocity = 0.03 m/s and solar radiation = 850 W/m²

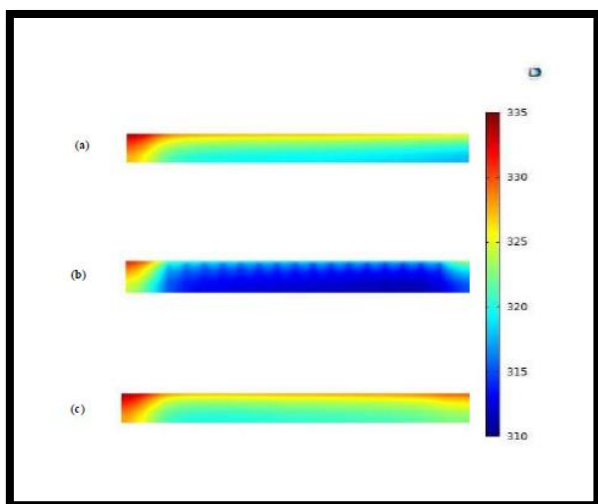


Figure 18. Cross section of a COMSOL simulation

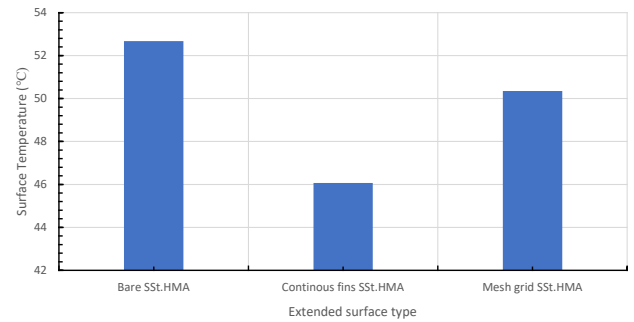


Figure 19. Surface temperature gathering line for all current cases at water velocity = 0.03 m/s and solar radiation = 850 W/m²

The variation in surface temperature values among ASC models is illustrated in Figure 19. As shown in this figure, the serpentine tubes provide a higher surface temperature than the finned tubes. It is clear that incorporating extended surfaces into ASC results in a decrease in its surface temperature, as recorded as (46.07°C) and (50.35°C) for the continuous finned and mesh grid serpentine tubes, respectively, when comparing with the bare serpentine tubes of (52.67°C).

It is found that the continuous fins model can capture more solar radiation than the mesh grid model by about 8.77%.

6. CONCLUSIONS

In this work, a low-carbon steel-alloy cheap waste materials have been investigated as a extended surface with HMA. ASC numerical model, which utilizes COMSOL Multiphysics, has been developed to include various types of extended surfaces inside ASC. The thermal effect of solar radiation is found to be insignificant in the HMA's lower layers. It is recognized that the extended surfaces have a noticeable thermal effect, increasing energy harvesting from HMA and thereby lowering its surface temperature. Finned serpentine tubes were found to be more effective than bare serpentine tubes in lowering the HMA's surface temperature. When extended surface techniques utilized, it is found that the maximum temperature reduction on the HMA surface is (6.6°C). In comparison to bare serpentine tubes, the surface temperatures of continuous finned and mesh grid tubes are (46.07°C) and (50.35°C), respectively. A maximum value of about 398.53 W can be gained (from a total of 850 W/m² incident solar radiation) by utilizing an extended surface. It is found that ASC efficiency increases from 66.74% for bare serpentine tubes to approximately 75.488% and 69.4% for continuous finned and mesh grid serpentine embedded tubes, respectively. For all models under investigation, it is clear that the optimum average Reynolds Number is about 600. It is found that the continuous fins model can capture more solar radiation than the mesh grid model by about 8.77%.

ACKNOWLEDGMENT

The authors would like to thank Mustansiriyah University (www.uomustansiriyah.edu.iq) in Baghdad-Iraq for its support in the current work.

REFERENCES

- [1] Budikova, D., Hogan, C., Hall-beyer, M., Hassan, G., Pidwirny, M. (2010). The Encyclopedia of Earth. Washington, DC: Environmental Information Coalition, National Council for Science and the Environment.
- [2] Wu, S., Chen, M., Zheng, J. (2011). Laboratory investigation into thermal response of asphalt pavements as solar collector by application of small-scale slabs. *Appl. Therm. Eng.*, 31(10): 1582-1587. <https://doi.org/10.1016/j.applthermaleng.2011.01.028>
- [3] Wang, H., Wu, S., Chen, M., Zhang, Y. (2010). Numerical simulation on the thermal response of heat-conducting asphalt pavements. *Phys. Scr. T*, 42(38).
- [4] Wong, N.H., Chen, Y. (2009). *Tropical Urban Heat Islands*. 1st ed., Taylor & Francis, Abngdon, UK.
- [5] Mallick, R.B., Chen, B.L., Bhowmick, S. (2009). Harvesting energy from asphalt pavements and reducing the heat island effect. *Int. J. Sustain. Eng.*, 2(3): 214-228. <https://doi.org/10.1080/19397038.2011.574742>
- [6] Brown, E.R., Cross, S.A. (1992). A national study of rutting in hot mix asphalt (HMA) pavements. <https://ntlrepository.blob.core.windows.net/lib/6000/6300/6383/rep92-05.pdf>.
- [7] Sullivan, C., de Bondt, A., Jansen, R., Verweijmeren, H. (2007). Innovation in the production and commercial use of energy extracted from asphalt pavements. 6th Annu. Int. Conf. Sustain. Aggregates, *Asph. Technol. Pavement Eng.*, p. 17.
- [8] Bobes-Jesus, V., Pascual-Muñoz, P., Castro-Fresno, D., Rodriguez-Hernandez, J. (2013). Asphalt solar collectors: A literature review. *Appl. Energy*, 102: 962-970. <https://doi.org/10.1016/j.apenergy.2012.08.050>
- [9] Khoja, A.O., Waheeb, S.A. (2016). Exploring the potentials of asphalt solar collectors in hot humid climates. *Innov. Energy Res.*, 5(2): 141.
- [10] Russell, R. (2007). Solar energy in earth's atmosphere.
- [11] Pan, T., Lu, Y., Wang, Z. (2012). Development of an atomistic-based chemophysical environment for modelling asphalt oxidation. *Polym. Degrad. Stab.*, 97(11): 2331-2339. <https://doi.org/10.1016/j.polymdegradstab.2012.07.032>
- [12] Sakka, A., Santamouris, M., Livada, I., Nicol, F., Wilson, M. (2012). On the thermal performance of low income housing during heat waves. *Energy Build.*, 49: 69-77. <https://doi.org/10.1016/j.enbuild.2012.01.023>
- [13] Webb, R.L., Kim, N. (2004). *Principles of Enhanced Heat Transfer*. 2th ed., Britain: Taylor and Francis Group.
- [14] Liu, X., Rees, S.J., Spitler, J.D. (2007). Modeling snow melting on heated pavement surfaces. Part I: Model development. *Appl. Therm. Eng.*, 27(5-6): 1115-1124. <https://doi.org/10.1016/j.applthermaleng.2006.06.017>
- [15] Wu, S., Li, B., Wang, H., Qiu, J. (2008). Numerical simulation of temperature distribution in conductive asphalt solar collector due to pavement material parameters. *Mater. Sci. Forum*, 575-578: 1314-1319. <https://doi.org/10.4028/www.scientific.net/MSF.575-578.1314>
- [16] Mallick, R., Chen, B., Bhowmick, S. (2009). Reduction of urban heat island effect through harvest of heat energy from asphalt pavements. 2nd Int. Conf. Countermeas. to Urban Heat Islands, pp. 1-20.
- [17] Basheer Sheeba, J., Krishnan Rohini, A. (2014). Structural and thermal analysis of asphalt solar collector using finite element method. *J. Energy*, 2014: 1-9. <https://doi.org/10.1155/2014/602087>
- [18] Mirzanamadi, R., Johansson, P., Grammatikos, S.A. (2018). Thermal properties of asphalt concrete: A numerical and experimental study. *Constr. Build. Mater.*, 158: 774-785. <https://doi.org/10.1016/j.conbuildmat.2017.10.068>
- [19] Zaim, E.H., Farzan, H., Ameri, M. (2020). Assessment of pipe configurations on heat dynamics and performance of pavement solar collector: An experimental study. *Sustainable Energy Technologies and Assessments*, 37: 100635. <https://doi.org/10.1016/j.seta.2020.100635>
- [20] Nicolas, S., Eleftherios, Z. (2010). Asphalt solar collector and borehole storage. Chalmers University of Technology.

NOMENCLATURE

ρ_{HMA}	Asphalt density (Kg/m ³)
cp_{HMA}	Asphalt specific heat (J/(Kg·°C))
K_{HMA}	Asphalt thermal conductivity (W/(m·°C))
n	Multiplier
G_o	Solar irradiation (W/m ²)
h_{amb}	Ambient heat transfer coefficient (W/m ² ·°C)
T_{amb}	Ambient temperature (°C)
$T_{HMA,S}$	Asphalt surface temperature (°C)
ρ_w	Water density (Kg/m ³)
cp_w	Water specific heat (J/(Kg·°C))
K_w	Water thermal conductivity (W/(m·°C))
$C_{u,w}$	Water heat capacity of x-axis (W/°C)
T_w	Water temperature (°C)
$u_{w,y}$	Velocity component of y-axis (m/s)
T_i	Water inlet temperature (°C)
$T_{initial}$	Initial temperature (°C)
ϵ	Emissivity
∇	The vector differential operator
α	Thermal diffusivity (m ² /s)

Abbreviation

UHI	Urban Heat Island
ASC	Asphalt Solar Collector
HMA	Hot Mixture Asphalt
C-HMA	Conductive Hot Mixture Asphalt
FEM	Finite Element Method
FDM	Finite Difference Method